JOURNAL OF APPLIED ELECTROCHEMISTRY 10 (1980) 627–634

Effects of radial diffusion on the efficiency of porous flow-through electrodes

B. G. ATEYA

Chemistry Department, Faculty of Science, Cairo University, Cairo, Egypt

Received 5 July 1979

A model is proposed to evaluate the effect of radial diffusion on the efficiency of porous flow-through electrodes. The model includes the electrode parameters of porosity (θ), thickness (L) and equivalent pore radius (R), the superficial flow speed of the electrolyte (v) and the molecular diffusivity of the reactant in the electrolyte (D). The effects of these variables are incorporated in a dimensionless group $\phi(L) = vR^2/2DL\theta$ which controls the conversion efficiency of the electrode. Satisfactory agreement was found between the model predictions and the experimental results of several authors on different electrode–electrolyte systems over a wide range of conditions. Implications of this work for design purposes are outlined. The effect of radial diffusion limitations on the voltage efficiency of the electrode is also discussed. It is shown that radial diffusion effects predominate under conditions of large values of pore radius, polarization and exchange current density, and small values of diffusivity.

List of symbols

b	RT/F (V)
c^0	Feed reactant concentration, (mol cm^{-3})
c_s	Reactant concentration at the electrode surface
$c(x)$	Average or 'mixing-cup' concentration of reactant at x
$c_m(x)$	Reactant concentration at the centre of the pore
$c_w(x)$	Reactant concentrations at the wall of the pore
d	Equivalent pore diameter (cm), Equation 2
D	Diffusion coefficient of reactant (cm^2 s^{-1})
f	Conversion efficiency of the electrode
i_L	Maximum obtainable limiting current, (A cm^{-2}) Equation 1
i_0	Exchange current density based on bulk concentration, c^0
i_0	Normalized exchange current density, i_0SL/i_L
L	Electrode thickness (cm)
n	Number of electrons
q	Tortuosity factor
R	Equivalent pore radius (cm)
(Re)	Reynolds number $(Re) = v/s\nu$
S	Specific surface area of the porous medium (cm^{-1})
(Sh)	Sherwood number $K_m d/D$
v	superficial flow speed (cm s^{-1})
x	Distance, see Fig. 3.
α	Transfer coefficient
$\eta(x)$	Polarization at distance x
θ	Porosity
$\phi(x)$	Dimensionless group, see Equation 6
ν	Kinematic viscosity (cm^2 s^{-1})

1. Introduction

The potential industrial applications of porous flow-through electrodes have recently generated considerable interest in this electrode system. It has been proposed for use in removing cyanide [1] and heavy metal ions [2–7] from industrial waste streams and in electrically rechargeable batteries for load-levelling applications [8]. The literature pertaining to this electrode system is expanding rapidly; adequate reviews have been recently published [9, 10].

The maximum limiting current obtainable from this electrode is given by

$$i_L = nFvc^0. \quad (1)$$

0021–891X/80/050627–08$02.80/0

There are several reasons why the electrode may not attain this value as discussed in the literature [10–23]. A major reason for this loss of efficiency is mass transfer restrictions in the radial direction. Under this condition the advantages of the electrode are not fully attained.

The conversion efficiency is defined as the ratio of the experimentally measured limiting current to that given by Equation 1. The dependence of this efficiency on flow speed and the structural parameters of the porous electrode is a question of prime importance for design purposes. Some authors [7, 12–20, 27] used an empirical approach to correlate the dependence of the experimental limiting current (and hence the conversion efficiency) on electrode thickness and electrolyte flow rate while others [3–6] used the empirical mass transfer coefficient obtained on packed beds [25] to treat the polarization effects in this electrode system. There are serious discrepancies between the empirical mass transfer coefficients reported by various workers [30, 31] including those using closely related techniques, e.g. the coefficients measured by Appel and Newman [26], Coeuret [27] and Sioda [28, 29] using porous flow-through electrodes are different from each other and from that of Wilson and Geankoplis [25]. Furthermore, such correlations shed no light on the mechanism of internal mass transfer and the discrepancies among them introduce uncertainties when used for design calculations.

In this paper an analytical solution for the conversion efficiency of the electrode is presented in terms of the superficial flow speed, reactant diffusivity and the structural parameters of the electrode, i.e. porosity, tortuosity, thickness and pore radius. The theoretical predictions are compared with the experimental results of many authors.

Radial diffusion has a second effect which is also related to the concentration gradient in the radial direction and to the voltage efficiency of the electrode. The latter is defined as [32]

$$\gamma_v = V/E$$

where E is the reversible thermodynamic electrode potential and V is the potential under operating conditions, i.e.

$$V = E - \sum \eta$$

where $\Sigma\ \eta$ is the sum of concentration, activation and ohmic polarizations. Thus, with slow radial diffusion, even if the conversion efficiency is unity, the reactant concentration at the pore wall $c_w(x)$ is less than that at the centre of the pore $c_m(x)$. The difference between $c_m(x)$ and $c_w(x)$ determines the extent of radial diffusion control and the magnitude of concentration polarization which affects γ_v. The second objective of this paper is to determine the dependence of the ratio $c_w(x)/c_m(x)$ on i_0, η, D and pore radius R (cf. under polarization effects).

2. Model, assumptions and solutions

The internal geometrical structure of a porous electrode is quite complicated and the electrode–electrolyte interface is difficult to describe exactly. However, a satisfactory treatment of the transport processes in such geometries may be achieved by using the concept of the 'equivalent diameter' which is defined by [33]

$$d = 4\theta/S \qquad (2)$$

where d is the equivalent pore diameter in cm, and S is the specific surface area of the porous medium in cm^{-1}. This approach proved useful in treating heat transfer problems in annular, triangular and rectangular conduits using cylindrical co-ordinates [33]. Alternatively, the porous matrix may be visualized as a large number of short tubular connections, randomly oriented. Consequently, the solutions for the concentration profile in a tube will be presented and then modified to account for porosity and tortuosity effects. We consider only the laminar flow regime for which experimental results are available. The flow is assumed laminar only in the general sense that the viscous forces predominate over the inertia forces [34]. The onset of turbulence is known to occur in porous media at $(Re) = 1$–10 [26].

There are two limiting cases of laminar flow in tubes: (a) Plug flow, which prevails in the velocity entrance region of straight tubes (or conduits), and (b) Fully developed (Poiseuille) flow which prevails in straight tubes and in artificial porous electrodes with straight cylindrical pores (or regions thereof). Inside a porous medium of regularly shaped particles under laminar flow, it is obvious that the velocity profile lies between these two limiting cases. Consequently, solutions are presented for both flow patterns for comparison with the experimental results.

The solution of the concentration distribution in a cylinder $c(x, r)$ with zero surface concentration throughout its length (corresponding to limiting current conditions) is readily available in the chemical engineering literature. The more useful concentration for the purpose of this work is the mean or 'mixing-cup' concentration, $c(x)$, which is obtained by averaging the concentration at a certain distance over the pore radius. This is given by Equations 3 and 4 for plug and parabolic velocity profiles, respectively [33].

$$c(x) = 4c^0 \sum_{i=1}^{i=\infty} (1/\xi_i)^2 \exp\left[-\xi_i^2 (xD/vR^2)\right] \tag{3}$$

$$c(x) = c^0 \sum_{j=1}^{j=\infty} \frac{-4B_j}{\beta_j^2} \left(\frac{d\psi_j}{dr}\right)_{r=R} \times \exp\left[-\beta_j^2 (2xD/vR^2)\right] \tag{4}$$

where ξ_i are the roots of the zeroth order Bessel function; i.e. $J_0(\xi_i) = 0$ and ψ_j, β_j and B_j are, respectively, the eigenfunction, the eigenvalue and a coefficient related to ψ_j. More details about these variables are available elsewhere [24].

The velocity of the electrolyte inside the pore (v_p) is related to the superficial velocity by [36] $v_p = vq/\theta$ where q is the tortuosity factor. Since $\theta < 1$ and $q > 1$, v_p must be several times greater than v; a factor of 4–8 was used in the petroleum engineering literature [37]. On the other hand, the true electrolyte path length x (true) $= xq$. Upon replacing x and v in Equations 3 and 4 by x (true) and v_p, and converting to dimensionless variables, one obtains

$$c(x)/c^0 = 4 \sum_{i=1}^{i=\infty} (1/\xi_i)^2 \exp\left[-\xi_i^2/2\phi(x)\right] \tag{5}$$

$$\frac{c(x)}{c^0} = \sum_{j=1}^{j=\infty} \frac{4B_j}{\beta_j^2} \left(\frac{d\psi_j}{dr}\right)_{r=1} \exp\left[-\frac{\beta_j^2}{4\phi(x)}\right] \tag{6}$$

where

$$\phi(x) = vR^2/2Dx\theta.$$

This dimensionless group includes the transport properties of the electrolyte and the structural properties of the electrode. The physical significance of $\phi(x)$ has been investigated before [23, 24].

3. The conversion efficiency

The conversion efficiency, f, is given by

$$f = 1 - c(L)/c^0 \tag{7}$$

The infinite series in Equation 3 and 5 converges rapidly for small $\phi(x)$ values. The first term is sufficient for $\phi(L) < 0.1$ whereas 50 terms are required for $\phi(L) = 1000$ for a relative error in f of $\leqslant 10^{-4}$. The lower roots of the zeroth order Bessel function were obtained from tables and the higher roots were calculated using [38]

$$\xi_i = (i - \tfrac{1}{4})\pi \qquad i \gg 1 \tag{8}$$

The first eleven terms of ψ_j, β_j and B_j are tabulated while higher terms were estimated using the relation [33]

$$\beta_j = 4(j-1) + 8/3 \qquad j = 1, 2, 3, \ldots \tag{9}$$

$$B_j = (-1)^{j-1}\, 2.846\, \beta_j^{-2/3} \tag{10}$$

$$-\frac{B_j}{2}\left(\frac{d\psi_j}{dr}\right)_{r=R} = 1.012\,76\, B_j^{-1/3} \tag{11}$$

The solid lines in Fig. 1 show the effect of the dimensionless group $\phi(L)$ on the conversion efficiency f for both plug and parabolic flow conditions, using Equation 3–7. The figure reveals the following:

(a) In the region of $\phi(L) > 1$, which corresponds to the developing concentration region [23], the predicted f is higher for plug flow than for parabolic flow; and

(b) As $\phi(L)$ decreases, f increases becoming ultimately equal to unity for $\phi(L) < 0.5$. This is the 'deep bed' region [33] in which the Sherwood number is a constant independent of position in the electrode (cf. under polarization effects). This is obtainable for electrodes of fine pores (small R) and large thickness (L), and/or reactants of high molecular diffusivity and low electrolyte flow rates.

4. Comparison with experimental results

The values of the conversion efficiency measured by various authors are compared with the calculated values in Fig. 1. Table 1 lists the relevant information for each set of results. The equivalent pore radius was calculated from the data reported by the various authors using Equation 2. The

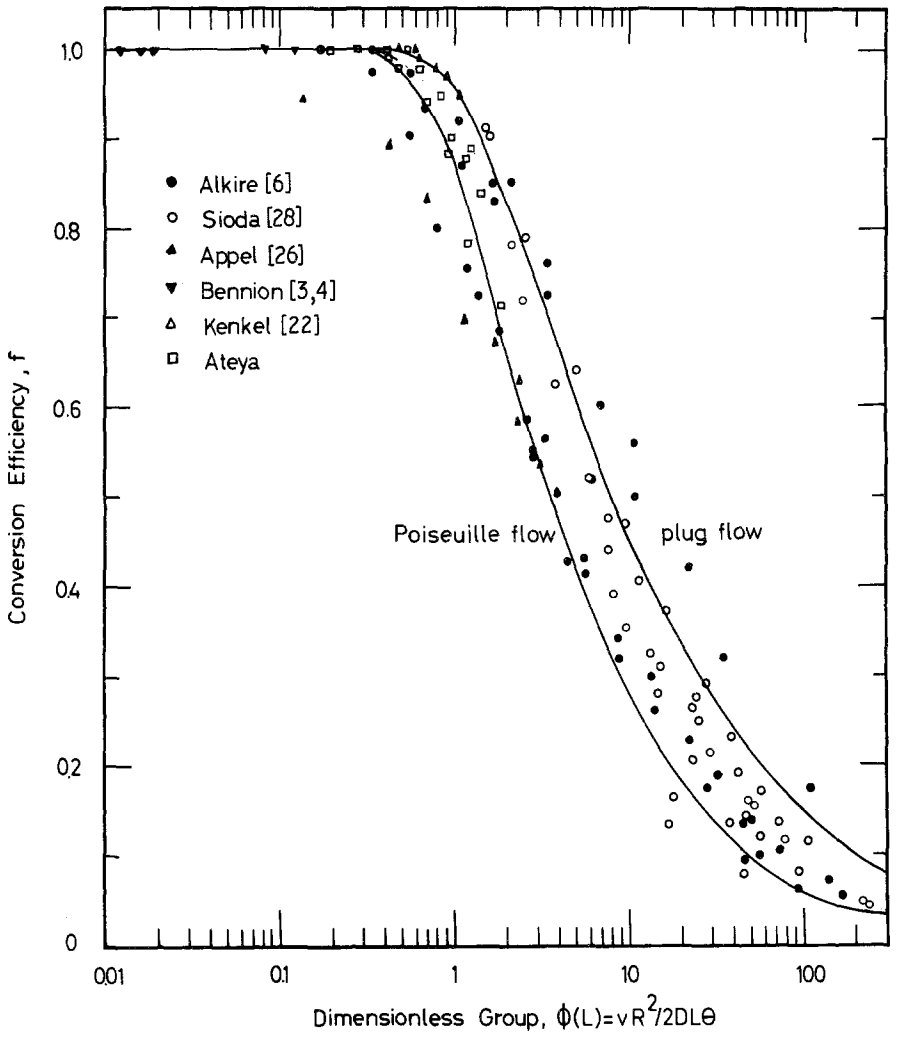

Fig. 1. Comparison of predicted and experimental efficiency relations.

values of the diffusion coefficient are: 7.6×10^{-6} cm^2 s^{-1} for the ferricyanide ion [39], 7.5×10^{-6} cm^2 s^{-1} for Cu^{2+} ions in 1.0 N H_2SO_4 [40], 5×10^{-6} cm^2 s^{-1} for Cu^{2+} ions in NH_4Cl–NH_4OH mixture [22] and 4×10^{-6} cm^2 s^{-1} for the ferric oxalate complex [41].

Inspection of Fig. 1 reveals the following:

(a) As $\phi(L)$ increases the efficiency decreases in accordance with the predictions of the model;

(b) A large number of the data points are enveloped between the Poiseuille flow curve (on the lower limit) and that of plug flow. This is quite satisfactory in view of the wide differences in the particle shape and size, electrode thickness and porosity, electrolyte flow rate, electrochemical and transport properties of the reactant system and the relative directions of electrolyte and current flow.

(c) A conversion efficiency of 100% is obtainable for $\phi(L) < 0.3$. This seems to be a safe design criterion. At lower efficiencies, the Poiseuille flow correlation slightly underestimates the efficiency and hence can be the basis for design calculations.

5. Polarization effects

Consider an electron transfer reaction, the rate of which is given by the Tafel equation including concentration effects i.e.

$$i = i_0(c_s/c^0) \exp(\alpha\eta/b) \qquad (12)$$

Table 1. Characterization of the electrode–electrolyte systems used by authors whose experimental results are used in Fig. 2

Authors	*Particle shape and dimensions*	*Porosity*	*Equivalent pore radius* (cm)	*Electrode thickness* (cm)	*Reaction*	*Range of* $\phi(L)$	*Range of* f	*Range of* (Re)
Appel and Newman [38]	Stainless steel spheres 4 mm diameter	0.37	0.078	1.06	reduction of ferricyanide in KNO_3	0.14–3.72	0.51–0.96	$< 0.046^*$
Sioda [12–20, 28]	Stacked 80 mesh Pt screens	0.80	0.016	0.025–0.18	reduction of ferricyanide in KCl	1–160	0.05–1	$< 1^*$
Bennion *et al.* [3, 4]	Carbon flakes of irregular shape	0.70	0.056	6	deposition of Cu^{2+} from 0.8 M Na_2SO_4	0.02–0.16	0.94–1.0	$< 0.01^*$
Alkire and Gracon [6]	Stacked 100 mesh Pt screens	0.64	0.006	0.03–0.7	ferro–ferricyanide in KCl; and deposition of Cu^{2+} from 3 N H_2SO_4	0.1–130	0.1–1.0	$\gtrsim 10^*$
Kenkel and Bard [22]	Sintered Ag disc	0.5	0.000 25	0.0050	reduction of Fe^{3+} in oxalate, and of Cu^{2+} in 1 M NH_4Cl–1 M NH_4OH	0.5–1.1	0.95–1.0	$< 0.05^\dagger$
Ateya	Packed Cu spheres	0.47	0.0147, 0.0106	2.1	Deposition of Cu^{2+} from 1 N H_2SO_4	0.1–2	0.7–1.0	$< 4^\ddagger$

Current and electrolyte flow: * parallel, † parallel and opposite, ‡ opposite.

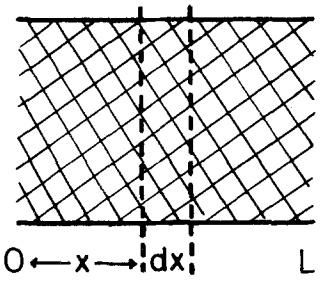

Fig. 2. Representation of the space element.

Performing a mass balance on a space element dx in Fig. 2, one obtains:

$$di(x) = i_0 S[c_w(x)/c^0] \exp[\alpha\eta(x)/b]\, dx. \quad (13)$$

This current increment is supported by radial diffusion the rate of which (cm^{-2} of internal pore area) is $k_m[c_m(x) - c_w(x)]$ where k_m is the mass transfer coefficient given by

$$k_m = (Sh)D/2R \quad (14)$$

Where (Sh) is the Sherwood number. For conditions of $\phi(L) < 0.5$ (i.e. $f \simeq 1$), (Sh) is a constant independent of distance inside the electrode and is 5.78 for plug flow and 3.56 for Poiseuille flow [33]. Thus

$$di(x) = nF[(Sh)DS/2R]\,[c_m(x) - c_w(x)]\, dx. \quad (15)$$

A complete description of the problem requires two more equations, namely a mass and a charge balance in the axial direction and the simultaneous solution of the four equations with the proper set of boundary conditions. This will be presented in a subsequent article and it will suffice here to solve the equations for the ratio of $c_w(x)/c_m(x)$. Thus, substituting for S from Equation 2, multiplying Equations 13 and 15 by L/v, equating and rearranging one obtains

$$\frac{c_w(x)}{c_m(x)} = \frac{1}{1 + [2\bar{i}_0\phi(L)(Sh)] \exp[\alpha\eta(x)/b]} \quad (16)$$

where $\bar{i}_0 = i_0 SL/i_L$ is the dimensionless normalized effective exchange current density of the electrode. Fig. 3 shows the variation of the concentration ratio $c_w(x)/c_m(x)$ with $\bar{i}_0\phi(L)$ and $\alpha\eta(x)$. It is evident that this ratio approaches unity for small values of $\bar{i}_0$, $\phi(L)$ and $\alpha\eta(x)$, i.e. low reaction rates, narrow pores, low electrolyte flow rates v and high values of reactant diffusivity D. This corresponds to conditions of negligible radial diffusion effects, i.e. $c_w(x)/c_m(x) > 0.9$. On the other hand $c_w(x)/c_m(x) < 0.1$ at high values of $\bar{i}_0$, $\phi(L)$ and $\alpha\eta(x)$, i.e. severe radial diffusion control under which condition radial diffusion is too slow to keep up with the reaction occurring at the pore walls and hence significant concentration polarization arises. Under this condition the one-dimensional models used by various authors to simulate the polarization behaviour of this electrode are expected to fail. Therefore the criterion for negligible radial diffusion control and for the validity of the one-dimensional models is

$$[2\bar{i}_0\phi(L)/(Sh)] \exp[\alpha\eta(x)/b] \ll 1. \quad (17)$$

The applicability of this criterion can best be illustrated by a numerical example. Thus for the condition of $\phi(L) = 0.5$, $\bar{i}_0 = i_0 SL/i_L = 0.1$, $(Sh) = 5.78$ and $\alpha\eta(x)/b = 3$, $c_w(x)/c_m(x) = 0.74$. This is only moderate radial diffusion control. An order of magnitude increase in $\bar{i}_0$ or in $\phi(L)$ makes this ratio equal to 0.22. An increase in $\alpha\eta(x)$ has a similar effect. On the other hand, a comparable decrease in $\bar{i}_0$, $\phi(L)$ or in $\alpha\eta(x)$ puts the system under conditions of negligible radial diffusion effects.

6. Conclusions

The agreement between the model predictions and the experimental results is quite satisfactory in some regions and is less so in others. To that extent the model, being an extension of an existing theory, is of more general applicability and hence is considered an improvement on the empirical or semi-empirical treatments of this system. The results of the model show clearly the domains of the various parameters where radial diffusion affects the conversion efficiency and how the latter is related to the structural parameters of the electrode and the transport properties of the electrolyte. Thus to achieve 100% conversion efficiency, a value of the dimensionless group $\phi(L) = vR^2/2DL\theta < 0.3$ is a safe value for design calculations.

The ultimate contribution of this work is that it presents a comparison between the experimental results of various authors and the prediction of a

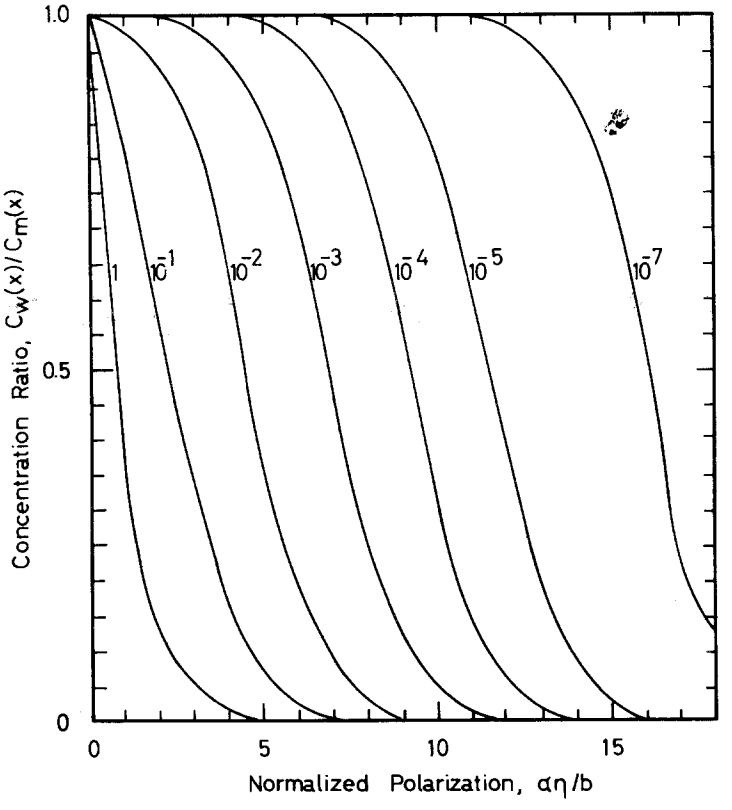

Fig. 3. Effect of the normalized polarization on, $c_w(x)/c_m(x)$. The numbers on the curves are $\bar{i}_0\phi(L)$.

well-known theoretical model within the framework of which one can easily visualize the interdependence of the factors which affect the conversion efficiency of the electrode. The treatment of polarization effects on $c_w(x)/c_m(x)$ enables one to evaluate the effects of $\bar{i}_0$, $\phi(L)$ and $\alpha\eta(x)$ on this concentration ratio. A criterion is developed for the validity of the one-dimensional models frequently used in analyzing the behaviour of this electrode system.

No mention is made in the above model or in previous ones of the effect of gas bubbles produced by a parasitic side reaction, e.g. H_2, O_2 or Cl_2 evolution. The evolution of such gases is likely to pose a serious problem for such models if the limiting current of the principal reaction occurs in a potential region in which it is both thermodynamically and kinetically favorable for the gas to evolve at a sufficient rate to form gas bubbles, i.e. beyond the saturation of the electrolyte with the gas. Under this condition the effective diffusion coefficient and the cross-sectional area available for electrolyte flow will be different from the respective values in the absence of the gas.

Although it can be easily appreciated that evolution of gas bubbles is accompanied by an increase in the former and a decrease in the latter, it is not possible at the present to estimate the extent of such variations due to the lack of pertinent information. In fact, experimental work in this area is called for to evaluate quantitatively the effect of gas bubbles on the above parameters and on the electrolyte flow speed. Therefore, the above model can be used for the cases either where no gas evolution occurs or where it occurs but the gas concentration in the electrolyte does not exceed its saturation value so that gas bubbles do not form.

Acknowledgement

The experimental results in [19, 20] were kindly supplied by R. Sioda in tabulated form.

References

[1] D. -T. Chin and B. Eckert, *Plating Surf. Finish.* October (1976) 38.

[2] A. T. Kuhn and R. W. Haughton, *ibid* **4** (1974) 69.
[3] D. N. Bennion and J. Newman, *J. Appl. Electrochem.* **2** (1972) 13.
[4] R. S. Wenger and D. N. Bennion, *ibid* **6** (1976) 385.
[5] J. A. Trainham and J. Newman, *ibid* **7** (1977) 287.
[6] R. Alkire and B. Gracon, *J. Electrochem. Soc.* **122** (1975) 1594.
[7] A. K. P. Chu, W. Fleischman and G. J. Hills, *J. Appl. Electrochem.* **4** (1974) 323.
[8] M. Warshay and L. O. Wright, *J. Electrochem. Soc.* **124** (1977) 173.
[9] J. Newman and W. Tiedman, *Amer. Inst. Chem. Eng. J.* **21** (1975) 25.
[10] J. Newman and W. Tiedman, 'Advances in Electrochemistry and Electrochemical Engineering', Vol. 11, (edited by H. Gerischer and C. Tobias), Wiley, New York (1978) p. 352.
[11] L. G. Austin, P. Palasi and R. Klimpel, 'Advances in Chemistry Series', no. 47, The American Chemical Society (1965) p. 35.
[12] R. E. Sioda, *Electrochim. Acta* **13** (1968) 375, 1559.
[13] *Idem*, *ibid* **15** (1970) 783.
[14] *Idem*, *ibid* **16** (1971) 1569.
[15] *Idem*, *ibid* **17** (1972) 1171, 1939.
[16] *Idem*, *ibid* **19** (1974) 57.
[17] *Idem*, *J. Appl. Electrochem.* **5** (1975) 221.
[18] *Idem*, *ibid* **7** (1977) 135.
[19] *Idem*, *J. Electroanalyt. Chem.* **34** (1972) 399, 411.
[20] *Idem*, *ibid* **70** (1976) 49.
[21] H. S. Wroblowa and G. Razumney, *J. Electroanalyt. Chem.* **49** (1974) 355.
[22] J. V. A. Kenkel and A. J. Bard, *ibid* **54** (1974) 47.
[23] B. G. Ateya, *ibid* **77** (1977) 183.
[24] B. G. Ateya, E. Arafat and S. A. Kafafi, *J. Appl. Electrochemistry* **7** (1977) 107.
[25] E. J. Wilson and C. J. Geankoplis, *Ind. Eng. Chem. Fund.* **5** (1966) 9.
[26] P. Appel and J. Newman, *Amer. Inst. Chem. Eng. J.* **22** (1976) 979.
[27] F. Coeuret, *Electrochim. Acta* **21** (1976) 185.
[28] R. E. Sioda, *ibid* **22** (1977) 439.
[29] R. E. Sioda, *J. Appl. Electrochem.* **8** (1978) 297.
[30] I. Colquhoun-Lee and J. Stepanek, *Chem. Eng. (London)* **282** (1974) 108.
[31] 'Chemical Engineers Handbook' (edited by R. H. Perry and C. H. Chilton) 5th edition, McGraw-Hill, New York (1973) p. 4–38.
[32] L. G. Austin, 'Handbook of Fuel Cell Technology' (edited by C. Berger) Prentice-Hall, N.J. (1968) p. 41.
[33] H. H. P. Skelland, 'Diffusional Mass Transfer', Wiley, New York (1974) pp. 142, 162, 287, 189, 485.
[34] S. S. Zabrodsky, 'Hydrodynamics and Heat Transfer in Fluidized Beds', M.I.T. Press, Cambridge (1966) p. 4.
[35] M. Muskat 'Physical Principles of Oil Production', McGraw-Hill, New York (1949) p. 126.
[36] S. J. Pirson, 'Oil Reservoir Engineering', 2nd ed. McGraw-Hill, New York (1958) p. 102.
[37] M. Muskat, 'The Flow of Homogeneous Fluids in Porous Media', J. W. Edwards, Michigan (1946) p. 62.
[38] F. Bowman, 'Introduction to Bessel Functions', Dover, New York (1958) p. 13.
[39] M. Eisenberg, C. W. Tobias and C. R. Wilke, *J. Electrochem. Soc.* **103** (1956) 413.
[40] W. Eversole, H. Kindswater and J. Peterson, *J. Phys. Chem.* **46** (1942) 370.
[41] R. De Leevwe, M. Sluyters-Rehback and J. H. Sluyters, *Electrochim. Acta* **14** (1969) 1183.